Enhanced Sb incorporation in InAsSb nanowires grown by metalorganic vapor phase epitaxy

Borg, Mattias; Dick Thelander, Kimberly; Eymery, Joel; Wernersson, Lars-Erik

Enhanced Sb incorporation in InAsSb nanowires grown by metalorganic vapor phase epitaxy

B. Mattias Borg,[1,a)] Kimberly A. Dick,[1,2] Joël Eymery,[3] and Lars-Erik Wernersson[1,4]

[1]*Solid State Physics, Lund University, Box 118, SE-221 00 Lund, Sweden*
[2]*Polymer and Materials Chemistry, Lund University, Box 124, SE-221 00 Lund, Sweden*
[3]*CEA Grenoble, INAC, SP2M, 17 rue des Martyrs, 38054 Grenoble, France*
[4]*Electrical and Information Technology, Lund University, Box 118, SE-221 00 Lund, Sweden*

We demonstrate metalorganic vapor phase epitaxy of $InAs_{1-x}Sb_x$ nanowires ($x=0.08-0.77$) for applications in high-speed electronics and long-wavelength optical devices. The composition of the InAsSb nanowires and InAsSb epilayers on the same sample is independently determined using lab-setup high resolution x-ray diffraction, by making use of the size-dependent in-plane broadening of the nanowire Bragg peak. We find that the incorporation of Sb into the nanowires is significantly higher than for planar epitaxy under the same growth conditions. Thermodynamic calculations indicate that this is due to a dramatically decreased effective V/III ratio at the particle/nanowire interface. © *2011 American Institute of Physics*. [doi:10.1063/1.3566980]

InAsSb-based photodiodes constitute an attractive and environment-friendly alternative to the HgCdTe detectors most commonly used for mid-infrared (IR) detection today. The InAsSb alloy has a band gap tunable throughout most of the mid-IR spectrum ($2-8$ μm) and can consequently be used for sensing of gases that are of importance to the environment, such as CO_2, CO, CH_4, N_2O, and O_3. A challenge for realizing InAsSb devices is that for most compositions of InAsSb, the available substrates give a very large lattice-mismatch, leading to a degradation of the material quality. One alternative is to grow nearly lattice-matched InAs/InAsSb or GaSb/InAs multiquantum wells, thus, realizing small effective band gaps via quantum confinement. However, these materials may suffer from rough heterointerfaces[1,2] and weak light absorption due to a spatial separation of the carriers.[3] The nanowire geometry is less sensitive to lattice-mismatch[4,5] and nanowire heterostructures with high lattice-mismatch (up to 15%) have been demonstrated with a maintained high crystal quality.[6] So far, reports on antimonide-arsenide alloy nanowires are sparse, focusing mostly on GaAsSb.[7,8] In this letter, we demonstrate metalorganic vapor phase epitaxy (MOVPE) of $InAs/InAs_{1-x}Sb_x$ heterostructure nanowires over a wide composition range ($x=0.08-0.77$). The chemical composition of the nanowires and the simultaneously grown epilayer is determined by high resolution x-ray diffraction (HRXRD) using a conventional lab-setup. These measurements are complemented by x-ray electron dispersed spectroscopy (XEDS) coupled with high-angle annular dark field scanning transmission electron microscopy (STEM).

Samples of epiready InAs(111)B wafers were prepared with Au aerosol nanoparticles of 50 nm diameter. InAs/InAsSb axial nanowire heterostructures were then grown by MOVPE, using trimethylindium (TMIn), trimethylantimony (TMSb), and arsine (AsH_3) as precursors. Before nanowire growth commenced, the sample was heated to 550 °C under AsH_3. InAs nanowire growth was induced by introducing

TMIn and AsH_3 into the reactor at 450 °C. To initiate the InAsSb nanowire growth, TMSb was added at various molar fractions. The molar fraction of a species is here defined as its volume flow divided by the total gas flow in the reactor (13 l/min). The V/III ratio during the InAsSb nanowire growth was set to 15, 27, or 56 by varying the group-V molar fractions while keeping the TMIn molar fraction constant at 4.7×10^{-6}. The incorporation of Sb into the InAsSb nanowires is investigated by varying the vapor phase composition, x_V, defined as

$$x_V = \frac{[TMSb]}{[TMSb] + [AsH_3]}, \tag{1}$$

where [x] is the molar fraction of the species x. The corresponding solid phase composition is $x=[Sb]/([Sb]+[As])$.

SEM images of typical InAs/InAsSb nanowires are shown in Figs. 1(a)–1(d), where the nanowires have increasing Sb content; $x=0.08$, 0.31, 0.53, and 0.77. The InAsSb segment is on top of the InAs segment and has a larger diameter than that of the InAs. This is similar to InSb and GaSb nanowire heterostructures,[9–11] for which the increased diameter is attributed mainly to an increased group-III concentration in the seed particle. Here, the diameter difference increases with x, and XEDS point analysis on single nanowires indicates a similar increase in the In content in the seed
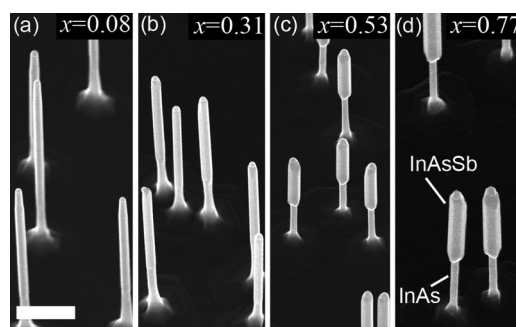

FIG. 1. SEM images taken at 30° tilt angle of $InAs/InAs_{1-x}Sb_x$ nanowires with increasing Sb content, $x=0.08$, 0.31, 0.53, and 0.77. The scale bar corresponds to 500 nm.

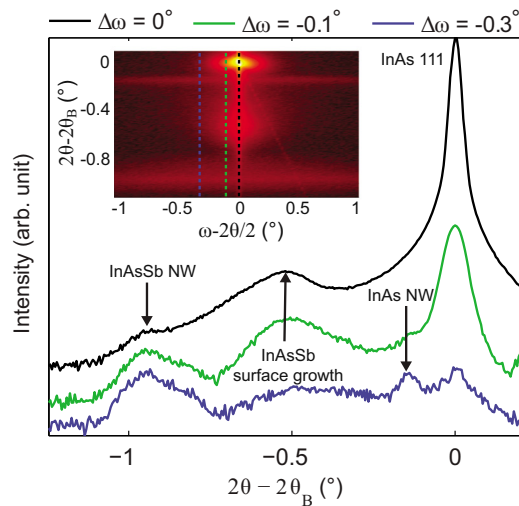a)Author to whom correspondence should be addressed. Electronic mail: mattias.borg@ftf.lth.se.

FIG. 2. (Color online) $2\theta/\omega$ scans near the 111-reflection of InAs, with varying $\Delta\omega$-offset. For finite offset the positions of the nanowire peaks are better resolved. The inset shows a map around the 111 InAs reflection, highlighting the much larger width of the nanowire peaks as compared to the peaks related to the surface growth and the substrate. The dashed lines indicate the position of the line-scans.

FIG. 3. (Color online) (a) Composition as measured by HRXRD of InAsSb nanowires and surface growth for various vapor composition (x_V), with nominal V/III ratio of 27. The Sb content (x) in the nanowires is significantly higher for all vapor compositions. (b) InAsSb nanowire solid composition for various x_V when grown with nominal V/III ratio=15, 27, and 56. For comparison, XEDS composition measurements are also shown for a few samples. The lines in (a) and (b) are the solutions of a thermodynamic calculation using only the V/III ratio as a variable parameter.

particles with increasing x, ranging from as low as 30% In (measured for x=0.12) up to 67% for x>0.5. The high In particle content in nanowires with high x matches the results of previous studies on InSb nanowires.[10,12] The solid composition of the InAsSb nanowire measured by XEDS is constant throughout most of the nanowire but is lower during the first 200 nm after the InAs/InAsSb interface. A few samples were also characterized by high resolution transmission electron microscopy (x=0.12–0.53), showing the structure to be zinc blende and without twin planes.

Lab-setup HRXRD of the 111 reflection was used to measure the solid composition of the as-grown InAsSb nanowires. In a standard measurement of the 111 crystal truncation rod, the detector (2θ) is scanned, while the sample-angle (ω) is kept at $\omega=2\theta/2$. For small x, the InAs substrate and InAsSb surface growth may hide the signal from the InAs$_{1-x}$Sb$_x$ nanowires, making it difficult to identify its exact position and shape (black line in Fig. 2). However, in this work we have added a small offset, $\Delta\omega$, to the ω-angle during the measurement ($\omega=2\theta/2+\Delta\omega$), thus separating the nanowire peak from the substrate and surface growth peaks (green and blue lines in Fig. 2). This method is based on the fact that nanowire diffraction peaks exhibit in-plane broadening due to the small crystal diameter. Consequently, nanowire peaks are normally much broader in the in-plane direction than both the substrate peak and the surface growth peak (inset of Fig. 2). Corresponding peak broadening has previously been used to determine the dimensions of quantum dots[13,14] and nanoparticles.[15]

Using the technique described above it was possible to independently determine the composition of the InAsSb nanowires and the InAsSb epilayer. The nanowires are assumed to be completely relaxed, based on the very short distance for the relaxation of strain in InP/InSb nanowires.[16] Complementary measurements of the 224 reflection were performed to determine the degree of relaxation and composition of the thin InAsSb epilayer. In Fig. 3(a) the solid composition of the InAsSb nanowires and the epilayer is compared for varying x_V (V/III ratio=27). It is clear that for most
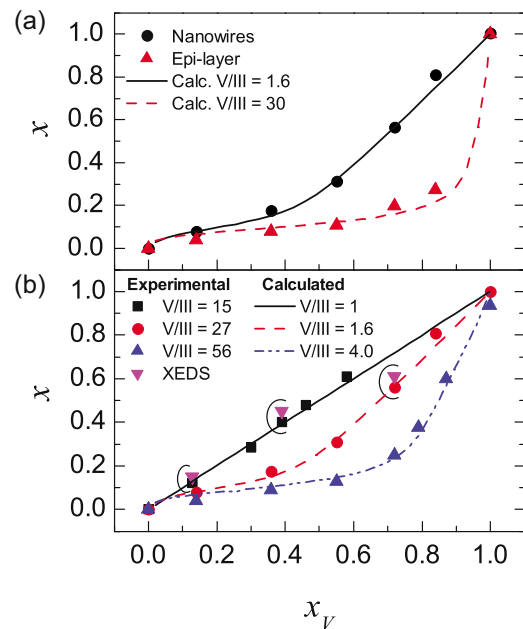
values of x_V, there is a significant enhancement in the amount of Sb incorporated into the nanowires compared to the epilayer. This result indicates a fundamental difference between the Sb incorporation during the InAsSb nanowire growth and planar epitaxy. XEDS investigations of single nanowires were also performed, to confirm the enhancement of Sb in the nanowires. The Sb composition as determined by XEDS is in fact slightly higher than that determined by HRXRD [Fig. 3(b)]. No variation in composition along the nanowire cross section could be measured, despite the appearance of lateral growth on the side facets.

To further explore these results, the V/III ratio during the InAsSb growth was varied between 15, 27, and 56 [Fig. 3(b)]. Our data shows that a reduction in the V/III ratio for constant x_V increases the incorporation of Sb into the InAsSb nanowires. This is in agreement with a previous study on MOVPE-grown InAsSb films, which shows that a V/III ratio of 1 or below is needed to acquire a unit solid-vapor distribution coefficient for Sb.[17] Here, the same trend is present, but a unit distribution coefficient is obtained already at a much higher V/III ratio (=15).

An established thermodynamic model, first applied to InAsSb by Biefeld[18] and similar to that used by Fukui and Horikoshi[19] fits well to the measured compositions of the epilayers [Fig. 3(a)] (dashed line). Values for the interaction parameter and chemical equilibrium constants were taken from Ref. 20. To agree with the measured nanowire compositions in Fig. 3(a), the V/III ratio in the calculation needs to be reduced to 1.6 (solid line). The same thermodynamic model was fitted to the experimental data of Fig. 3(b) and gave best agreement with V/III ratio of 1, 1.6, and 4.0 for nominal V/III ratio of 15, 27, and 56. In all three cases, this

means roughly 15 times lower values than the nominal V/III ratios.

To explain the discrepancy between the nominal and apparent V/III ratio we consider the Au:In:As:Sb seed particle on top of the nanowire. The composition of the nanowire is determined by the chemistry at the interface between the particle and the crystal, and the composition of, and diffusion rates through, the seed particle will thus be of great importance for the composition of the grown nanowire. The observed high In content of the seed particle post-growth suggests that it acts as an In reservoir during growth, and thus strongly reduces the effective V/III ratio at the growth interface, as compared to the surrounding vapor. This increases the Sb incorporation of the nanowire growth.

In conclusion, we have demonstrated InAsSb nanowire growth by MOVPE over a wide composition range (0.08 < x < 0.77). The realization of InAsSb nanowires with high Sb content is an important step toward realizing efficient mid-IR optoelectronic devices. The composition of the InAsSb nanowires and InAsSb epilayers was simultaneously determined using lab-setup HRXRD, by making use of the size-dependent in-plane broadening of the nanowire Bragg peak. The incorporation of Sb in the nanowires is significantly higher than for planar epitaxy under the same conditions, possibly due to a dramatically decreased effective V/III ratio at the particle/nanowire interface. This result highlights a fundamental difference between planar and nanowire epitaxy and is an experimental verification that the seed particle can strongly alter the precursor stoichiometry during nanowire growth.

[1] D. Lackner, O. J. Pitts, S. Najami, P. Sandhu, K. L. Kavanagh, A. Yang, M. Steger, M. L. W. Thewalt, Y. Wang, D. W. McComb, C. R. Bolognesi, and S. P. Watkins, J. Cryst. Growth **311**, 3563 (2009).
[2] R. M. Feenstra, D. A. Collins, D. Z.-Y. Ting, M. W. Wang, and T. C. McGill, Phys. Rev. Lett. **72**, 2749 (1994).
[3] H. Kroemer, Physica E (Amsterdam) **20**, 196 (2004).
[4] F. Glas, Phys. Rev. B **74**, 121302 (2006).
[5] L. C. Chuang, M. Moewe, C. Chase, N. P. Kobayashi, and C. Chang-Hasnain, Appl. Phys. Lett. **90**, 043115 (2007).
[6] P. Caroff, M. E. Messing, B. M. Borg, K. A. Dick, K. Deppert, and L.-E. Wernersson, Nanotechnology **20**, 495606 (2009).
[7] S. Plissard, K. A. Dick, X. Wallart, and P. Caroff, Appl. Phys. Lett. **96**, 121901 (2010).
[8] D. L. Dheeraj, G. Patriarche, L. Largeau, H. L. Zhou, A. T. J. van Helvoort, F. Glas, J. C. Harmand, B. O. Fimland, and H. Weman, Nanotechnology **19**, 275605 (2008).
[9] L. Lugani, D. Ercolani, F. Rossi, G. Salviati, F. Beltram, and L. Sorba, Cryst. Growth Des. **10**, 4038 (2010).
[10] P. Caroff, J. B. Wagner, K. A. Dick, H. A. Nilsson, M. Jeppsson, K. Deppert, L. Samuelson, L. R. Wallenberg, and L.-E. Wernersson, Small **4**, 878 (2008).
[11] M. Jeppsson, K. A. Dick, J. B. Wagner, P. Caroff, K. Deppert, L. Samuelson, and L.-E. Wernersson, J. Cryst. Growth **310**, 4115 (2008).
[12] D. Ercolani, F. Rossi, A. Li, S. Roddaro, V. Grillo, G. Salviati, F. Beltram, and L. Sorba, Nanotechnology **20**, 505605 (2009).
[13] B. Krause and T. H. Metzger, Phys. Rev. B **72**, 085339 (2005).
[14] I. Kegel, T. H. Metzger, A. Lorke, J. Peisl, J. Stangl, G. Bauer, J. M. Garcia, and P. M. Petroff, Phys. Rev. Lett. **85**, 1694 (2000).
[15] A. L. Patterson, Phys. Rev. **56**, 978 (1939).
[16] V. Favre-Nicolin, F. Mastropietro, J. Eymery, D. Camacho, Y. M. Niquet, B. M. Borg, M. E. Messing, L.-E. Wernersson, R. E. Algra, E. P. A. M. Bakkers, T. H. Metzger, R. Harder, and I. K. Robinson, New J. Phys. **12**, 035013 (2010).
[17] R. M. Biefeld, J. Cryst. Growth **77**, 392 (1986).
[18] R. M. Biefeld, J. Cryst. Growth **75**, 255 (1986).
[19] T. Fukui and Y. Horikoshi, Jpn. J. Appl. Phys., Part 2 **19**, L53 (1980).
[20] M. B. Panish and M. Illegems, Prog. Solid State Chem. **7**, 39 (1972).